**Constraining the Hydration of X-ray Amorphous and Clay Mineral Phases in Gale Crater, Mars.** S. Czarnecki[1], C. Hardgrove[1], E. B. Rampe[2], R. J. Smith[3], and P. J. Gasda[4] [1]Arizona State University, Tempe, AZ (sean.czarnecki@asu.edu), [2]NASA Johnson Space Center, Houston, TX, [3]SUNY Stony Brook, Stony Brook, NY, [4]Los Alamos National Lab, Los Alamos, NM.

**Introduction:** Clay minerals and salts in the Gale crater stratigraphy investigated by the Mars Science Laboratory (MSL) *Curiosity* rover preserve information about sediment sources, depositional environment, and post-depositional alteration. Amorphous component compositions have bearing on the redox potential, pH, and chemistry of alteration fluids, and on the heterogeneity of these conditions [e.g., 1]. Interlayer clay hydration in present-day Gale crater could indicate high water/rock ratios of late-stage fluid alteration events, increasing the potential habitability of post-depositional environments [1]. The MSL Dynamic Albedo of Neutrons instrument (DAN) measures bulk hydration, and here we attempt to determine the hydration of clay minerals and amorphous components throughout the *Curiosity* traverse to constrain the abundance of individual amorphous phases and determine if clay interlayer water is present today. The implications will also be more broadly applicable to sedimentary successions beyond the MSL traverse.

In this study, we compare hydration results from DAN to mineralogical results from the MSL Chemistry and Mineralogy instrument (CheMin) for 16 different sample locations. CheMin typically measures one or more hydrated crystalline phases, a hydrated X-ray amorphous fraction composed of multiple phases, and one or more collapsed (i.e., no interlayer water) clay mineral phases. However, Gale samples are known to dehydrate during sample acquisition and handling [2], and because DAN measures hydration to a depth of tens of cm, we can test for the presence of clay interlayer water *in situ* by comparing DAN bulk hydration to CheMin mineralogy. We can also constrain the hydration of the amorphous fractions, and with chemistry from the ChemCam and APXS instruments, this will allow us to better define the amorphous phases.

**Instruments:** DAN is a neutron spectrometer which pulses 14.1 MeV neutrons at 10 Hz and counts thermal ($\leq$ 0.3 eV) and epithermal (0.3 eV < n < 100 keV) neutrons returning from the top ~50 cm of the subsurface in a few meters laterally [3]. Counts are tabulated by a time-of-flight "die-away" curve, the shape of the curve depending on subsurface chemistry. DAN is sensitive to hydrogen [e.g., 3], which increases thermal neutron counts, and bulk thermal neutron absorption cross section, $\Sigma_{abs}$, which reduces thermal neutron counts. $\Sigma_{abs}$ is the weighted sum of the cross sections of all neutron absorbers (e.g., Cl, Fe) [4].

CheMin is an X-ray diffraction instrument which determines mineralogical abundances of powdered samples drilled from depths of a few cm [5]. CheMin results include abundances of well-crystalline minerals as well as clay minerals and amorphous components.

**Methods:** We compare the shape of DAN die-away curves to die-away curves simulated using MCNP6 software [6]. MCNP6 simulates neutron histories in a 3D environment which models the rover, atmosphere, and subsurface chemistry. We create a "grid" of subsurface models by independently varying hydrogen abundance and $\Sigma_{abs}$. The ranges we use for hydrogen and $\Sigma_{abs}$ are representative of measurements along the MSL traverse [7]. In this work we use homogeneous models, assuming that hydrogen and $\Sigma_{abs}$ do not vary laterally or vertically within the DAN field of view. We then use a Markov-chain Monte-Carlo analysis to determine a best-fit mean value for each parameter with associated uncertainties [8,9]. Hydrogen abundance results are reported in units of wt.% WEH (water-equivalent hydrogen), obtained by converting a best-fit hydrogen abundance into a corresponding water abundance.

We identified DAN active measurements which best correspond to CheMin drill samples. In some cases, the DAN measurements were taken directly over the drill site; for others they were taken within a few meters of the drill site. Some locations had multiple DAN measurements equidistant from the same drill site, and for these we have taken the mean value of the DAN results. In a few cases, where multiple samples were obtained within a radius of a few meters of one DAN measurement, we took the mean CheMin mineral abundances for comparison with DAN results.

Crystalline phases are well-constrained by CheMin, which is also typically able to identify the specific clay mineral phase(s), constraining the abundance of structurally-bound hydroxyl. We use the following equation to subtract the WEH due to $OH^-$ and $H_2O$ in crystalline phases and structural $OH^-$ in clay minerals to calculate the quantity $WEH_{aci}$, which is the amorphous fraction hydration + clay interlayer water hydration:

$$WEH_{aci} = WEH - \sum WEH_{min_i}[min_i] - WEH_c[clay]$$

where $WEH \equiv$ bulk WEH, $[min_i] \equiv$ abundance of the $i$th mineral phase.

**Results:** $WEH_{aci}$ includes both interlayer clay hydration and amorphous component hydration, both of

which depend on the composition of the component phases. Several different clay minerals have been identified based on CheMin XRD data, and water retention capability varies among clays. Clay minerals identified include ferrosaponite (Fe-sap) [10,11], ferripyrophyllite (Fe-prl) [12,13], mixtures of Al-montmorillonite and Mg-saponite (Al-mm/Mg-sap) [12], and nontronite [14].

We plotted $WEH_{aci}$ as a function of both amorphous fraction (Fig. 1) and clay fraction (Fig. 2), symbolized by clay mineral. Fe-sap and Fe-prl samples follow similar trends in both plots, whereas Al-mm/Mg-sap samples follow a similar trend to Fe-sap and Fe-prl in the clay plot, but a different trend in the amorphous plot. Similarly, nontronite samples follow a similar trend to Fsap and Fprl in the amorphous plot, but a different trend in the clay plot. Based on this, we proceed with a Fe-sap and Fe-prl category (Fe-sap/Fe-prl), with separate categories for Al-mm/Mg-sap and nontronite.

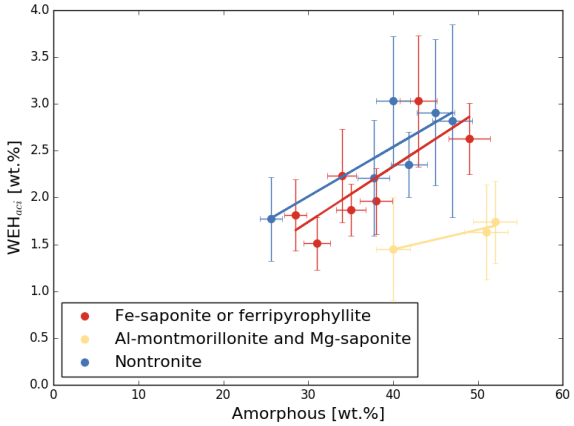


*Figure 1: DAN $WEH_{aci}$ as a function of CheMin amorphous component wt.% for three categories of clay minerals.*

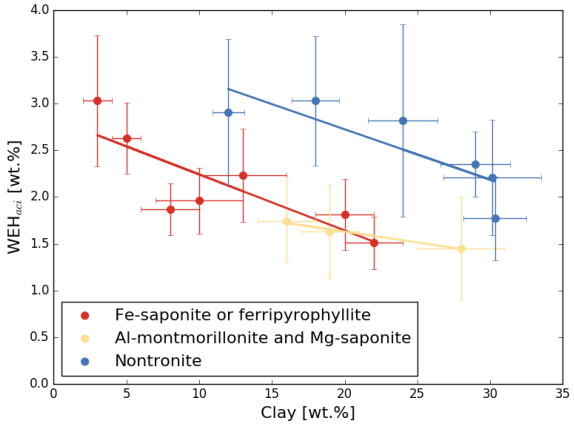


*Figure 2: DAN $WEH_{aci}$ as a function of CheMin clay mineral wt.% for three categories of clay minerals.*

Fig. 2 shows negative trends between $WEH_{aci}$ and clay abundances. This could be explained by a positive trend between $WEH_{aci}$ and amorphous abundance (Fig. 1), and that samples with more clay tend to contain less amorphous material. However, the significantly greater $WEH_{aci}$ of nontronite samples from the Glen Torridon region in comparison to the other samples [15] could indicate nontronite is hydrated in these samples. Alternatively, the elevated $WEH_{aci}$ of nontronite samples could indicate that the amorphous phases in these samples are more hydrated than the amorphous phases in other samples. An amorphous component analysis which accounts for the chemistry and hydration of the amorphous fraction could determine this [9].

**Discussion:** CheMin XRD results have consistently shown fully dehydrated clay minerals in all clay-bearing samples [10-14]. However, the possibility of remnant interlayer water in a few samples and the known dehydration of other phases during sample handling suggests that clay minerals in Gale crater could still be hydrated in the subsurface. DAN is uniquely suited to address this question because it measures hydration of material *in situ*. Although the trends in Fig. 2 suggest that clay minerals are not hydrated in the subsurface, the large abundance of nontronite in Glen Torridon samples [14] and the greater hydration of these samples [15] could indicate that these clay minerals are hydrated.

This work will proceed with an amorphous component analysis to put constraints on individual amorphous phases. The composition of the amorphous fraction can shed light on the redox potential, pH, and chemistry of past alteration fluids. This analysis may also constrain the hydration of nontronite in Glen Torridon samples.

**Acknowledgments:** The authors would like to thank the MSL science team, as well as Foteine Dimitracopoulos for helpful comments. Support was provided by the MSL Participating Scientist Program. All data used are available on the NASA PDS.
pds-geosciences.wustl.edu/missions/msl/dan.htm
pds-geosciences.wustl.edu/missions/msl/chemin.htm

**References:** [1] McAdam, A.C., et al. (2022) *JGR: Planets*, 127. [2] Rapin, W., et al. (2018) *JGR: Planets*, *123*. [3] Mitrofanov, I. G., et al. (2012) *Space Sci. Rev., 170*, 559-582. [4] Hardgrove, C., et al. (2011) *NIMA, 659*, 442-455. [5] Blake, D., et al. (2012) *Space Sci. Rev., 170*, 340-391. [6] Werner, C. J., et al. (2018) MCNP user's manual: Code version 6.2. LA-UR-17-29981. [7] Kerner, H.R., et al. (2020) *JGR: Planets, 125*. [8] Foreman-Mackey, D., et al. (2013) *Publications of the Astronomical Society of the Pacific 125 (925)*, 306-312. [9] Gabriel, T. S. J. et al. (2018) *GRL, 45*. [10] Vaniman, D.T., et al. (2014) *Science, 243* [11] Rampe, E.B., et al. (2017) *EPSL, 471*, 172-185. [12] Bristow, T.F., et al. (2018) *Sci. Adv., 4*. [13] Rampe, E.B., et al. (2020) *JGR: Planets, 125*. [14] Thorpe, M. T., et al. (2022) *JGR: Planets, 127*. [15] Czarnecki, S., et al. (2023) *JGR: Planets, accepted.*